On decoupling of volatility smile and term structure in inverse option pricing

Herbert Egger[1], Torsten Hein[2] and Bernd Hofmann[2]

[1] Center for Computational Engineering Science (CCES), RWTH Aachen, Pauwelstraße 19, D-52074 Aachen, Germany
[2] Department of Mathematics, Chemnitz University of Technology, Reichenhainer Str. 41, D-09107 Chemnitz, Germany

E-mail: egger@mathcces.rwth-aachen.de, thein@mathematik.tu-chemnitz.de and hofmannb@mathematik.tu-chemnitz.de

Abstract

Correct pricing of options and other financial derivatives is of great importance to financial markets and one of the key subjects of mathematical finance. Usually, parameters specifying the underlying stochastic model are not directly observable, but have to be determined indirectly from observable quantities. The identification of local volatility surfaces from market data of European vanilla options is one very important example of this type. As with many other parameter identification problems, the reconstruction of local volatility surfaces is ill-posed, and reasonable results can only be achieved via regularization methods. Moreover, due to the sparsity of data, the local volatility is not uniquely determined, but depends strongly on the kind of regularization norm used and a good *a priori* guess for the parameter. By assuming a multiplicative structure for the local volatility, which is motivated by the specific data situation, the inverse problem can be decomposed into two separate sub-problems. This removes part of the non-uniqueness and allows us to establish convergence and convergence rates under weak assumptions. Additionally, a numerical solution of the two sub-problems is much cheaper than that of the overall identification problem. The theoretical results are illustrated by numerical tests.

(Some figures in this article are in colour only in the electronic version)

1. Introduction

Stochastic models for the evolution of financial assets are at the core of mathematical finance. In the famous Black–Scholes model [1], a financial asset, e.g. a stock S, is assumed to follow the geometric diffusion

$$dS_t = \mu S_t \, dt + \sigma S_t \, dW_t, \tag{1}$$

with drift rate μ and volatility σ. Here, W_t denotes a Brownian motion. For details on mathematical finance we refer to [14, 19] and the references cited therein. Using no arbitrage arguments and Ito calculus, one can show that the value of a European call option on an asset following (1) has to satisfy the (Black–Scholes) partial differential equation

$$C_t + \tfrac{1}{2}\sigma^2 S^2 C_{SS} + rSC_S - rC = 0, \tag{2}$$

where r is the short-term interest rate. As a consequence of no arbitrage arguments r enters (2) instead of μ. The value of a European call option $C = C(S, t; K, T)$ with strike K and maturity T at maturity $t = T$ is given by the payoff

$$C(S, T; K, T) = \max(S - K, 0). \tag{3}$$

Under the assumption that the coefficients σ and r are constants (2), (3) admit an analytic solution (the famous Black–Scholes formula, cf [1]). The interest rates r can usually be determined from other financial instruments and are assumed to be known here. Hence, the model (1) is specified by the single parameter σ, which can be uniquely determined from one single option price depending monotonically on σ. The unique level of volatility corresponding to an option price is also called (Black76) implied volatility.

A major drawback of the simple Black–Scholes model (1) is that the assumption of a constant volatility in most situations contradicts market observations, i.e. implied volatilities corresponding to options with different strikes K and maturities T are not constant, but typically depend on K and T, which is known as the smile effect [5]. Consistency with the market can be restored by using a volatility function $\sigma(S, t)$ instead of a constant, see [6]. In order to specify a stochastic model (1) which is consistent with the market, a local volatility function $\sigma(S, T)$ has to be found such that quoted market prices $C^*(K, T) = C(S_0, 0; K, T)$ are matched. As for constant parameters C has to solve (2), (3), and S_0 denotes the spot price of the underlying asset S and $t = 0$ meaning today. Once the volatility function has been determined, many different financial derivatives depending on S can be priced using (2) or similar equations.

Due to its relevance in practice, the following *inverse problem of option pricing (IPOP)*, also known as *market calibration*, has attracted significant interest in the past.

Inverse problem 1.1 (IPOP). *Given prices $C^*(K, T)$ of European call options, find a volatility function $\sigma(S, T)$ such that the solutions C of the Black–Scholes equation (2) satisfy the calibration condition $C(S_0, 0; K, T) = C^*(K, T)$ for all (given) K and T.*

In [17], the authors use a spline representation of the volatility surface $\sigma(S, t)$ and propose to solve the parameter identification problem corresponding to (2) by a regularized least-squares approach. Note that in (2) the dependence of the option values on strikes K enter via the terminal condition (3), which complicates the analysis and numerical solution of the inverse problem. As shown in [3, 6], prices of European call options alternatively satisfy the Dupire equation

$$\begin{aligned}
C_T &= \tfrac{1}{2}\sigma^2(K, T)K^2 C_{KK} - rKC_K, &\quad (K, T) &\in \mathbb{R}_+ \times (0, T^*], \\
C(S_0, 0; K, 0) &= \max(S_0 - K, 0), &\quad K &\in \mathbb{R}_+,
\end{aligned} \tag{4}$$

where T^* denotes the maximal time horizon (maturity) of interest respectively for which option prices are available. Hence, the inverse problem of option pricing can be seen as a parameter identification problem for the parabolic equation (4). As with many parameter identification problems the inverse problem 1.1, specifically the identification of $\sigma(K, T)$ in (4), is ill-posed (see [7]) i.e. a solution does not depend stably on the data and the problem can only be solved by some regularization method. Stable recovery of the volatility function $\sigma(K, T)$ from observed option prices $C^*(K, T)$, which can be considered as noisy data of

solutions $C(K, T)$ to the Dupire equation, has been investigated previously by several authors; see, e.g. [2, 4, 7, 12, 16, 18].

However, an important aspect that has been neglected in most of the previous works is the specific data situation. Typically, option prices are available for a relatively large number of strikes K but only a few maturities T. Additionally, a stable determination of volatilities for high/low strikes is only possible for relatively large maturities, and thus the reconstructions for short maturities will depend highly on initial values with respect to the kind of regularization used in the least-squares approach. In order to incorporate the special data situation, an ansatz

$$\sigma(K, T) = \sigma(K)\rho(T)$$

was proposed in [3]. In the present paper, we will use a similar decomposition of volatility smile and term structure, namely

$$\sigma(K, T) = \sigma_1\big(e^{-\int_0^T r(t)\,dt} K\big)\sigma_2(T) \tag{5}$$

and show that such a decomposition has several advantages.

First of all, by the special choice (5), the parameter identification problem decomposes into two separate sub-problems, i.e., the term and smile structure can be determined separately. The cases of a purely price-dependent and purely time-dependent volatility have been investigated in detail previously, see, e.g., [3, 7, 12, 18, 20], and parts of the theoretical considerations also apply to our situation. For the stable solution of the sub-problems we propose and analyse regularized least-squares approaches, i.e., Tikhonov regularization. We will derive our theoretical results with minimal requirements on the data, i.e., we show that the volatility smile σ_1 can be determined from option prices for only one maturity, while the term structure σ_2 can be recovered from option data for only one strike. Our inverse problem is the following:

Inverse problem 1.2 (Decoupled IPOP). *Let* $C_1(K) := C^*(K, T^*)$, $C_2(T) := C^*(K^*, T)$ *denote option prices for fixed maturity* T^* *respectively fixed strike* K^*. *Determine functions* $\sigma_1(\cdot)$, $\sigma_2(\cdot)$ *such that the solution* $C(K, T)$ *to (4) with* $\sigma(K, T)$ *defined by (5) satisfies*

$$C(K, T^*) = C_1(K), \quad K \in \mathbb{R}_+ \qquad and \qquad C(K^*, T) = C_2(T), \quad T \in [0, T^*].$$

Although, from an analytical point of view, option prices C_1 for all strikes and one maturity, respectively C_2 for one strike and all maturities are sufficient for determining the smile and term structure σ_1, σ_2, all available option prices can be utilized for the sub-problems alternatively, which may additionally stabilize their solution.

Remark 1.1. The volatility smiles $\sigma(\cdot, T)$ for maturities T depend on discounted strikes: this makes sense from a practical point of view, since volatility smiles usually attain their minimum near the spot $K = S(t)$, i.e. they *float* with evolving time.

One of the conjectures against an assumption of a special structure (5) of volatility might be that the implied volatility smiles usually flatten over time. However, as we will show by our numerical experiments, such a behaviour is not in contradiction to our assumption on the structure of the volatility, i.e. the Black76 volatilities corresponding to the volatility surface (5) also show this flattening phenomenon.

Finally, as we will outline in more detail in section 5, the assumption of the special form (5) allows a fine discretization and thus good resolution of the local features of the volatility smile, and a fast numerical solution of the identification problem at the same time. Even in case that the true volatility does have a different form than (5), a reconstructed volatility of the form (5) may serve as a good initial guess for the general inverse problem 1.1.

The outline of the paper is as follows. In the following section, we formulate the inverse problem in more detail and show that, for a volatility surface of the form (5), the calibration naturally decomposes into the two sub-problems of recovering the smile and the term structure separately. In section 3, we discuss the problem of identifying the smile and recall the most important results on its regularization and stable solution. The problem of recovering the term structure will be investigated in section 4. Finally, we discuss some details of an efficient numerical implementation and present the results of numerical tests in section 5.

2. Decoupling of the smile and term structure

We are concerned here with the identification of a local volatility function $\sigma(K, T)$ in the Dupire equation from market observations $C^*(K, T)$ of option prices satisfying the Black–Scholes equation (2). Due to the limited availability of data, we restrict the class of admissible volatilities to the form such as (5), i.e. we assume the volatility smile to float with discounted strikes $Y = e^{-\int_0^T r(t)\,dt} K$. In order to make the decomposition into the smile σ_1 and term structure σ_2 unique, we set

$$\int_0^{T^*} \sigma_2^2(t)\,dt = 1, \tag{6}$$

where T^* denotes the largest maturity for which option prices are taken into account. We show now that by a transformation of variables the inverse problem decomposes rather naturally into two separate sub-problems.

Let $A(Y) = \frac{1}{2}\sigma_1^2(Y)$ and $B(T) = \sigma_2^2(T)$ denote the smile and term structure of volatility. By a rescaling of time, namely

$$\tau(T) := \int_0^T B(t)\,dt, \tag{7}$$

and with the notation $U(Y, \tau) := C(K, T)$, the Dupire equation (4) transforms into

$$\begin{aligned}
U_\tau(Y, \tau) &= A(Y)Y^2 U_{YY}(Y, \tau), & (Y, \tau) &\in (0, \infty) \times (0, 1] \\
U(Y, 0) &= \max(S_0 - Y, 0), & Y &\in (0, \infty),
\end{aligned} \tag{8}$$

where we used that $\int_0^{T^*} B(t)\,dt = 1$ by (6). The degeneracy in (8) can be lifted by transformation into *logarithmic* variables $y = \log(Y)$, which yields

$$\begin{aligned}
u_\tau(y, \tau) &= a(y)(u_{yy}(y, \tau) - u_y(\tau)), & (y, \tau) &\in \mathbb{R} \times (0, 1], \\
u(y, 0) &= \max(S_0 - e^y, 0), & y &\in \mathbb{R},
\end{aligned} \tag{9}$$

where $a(y) = A(Y)$ and $u(y, \tau) = U(Y, \tau)$. Using standard theory for parabolic equations one gets the following result (see [2]):

Proposition 2.1. *Let $A(Y) \in C^\lambda(\overline{\mathbb{R}_+})$ for some $\lambda \in (0, 1)$. Then (8) has a unique solution $U \in C^{2,1}(\mathbb{R}_+ \times (0, T^*]) \cap C^{\lambda,\lambda/2}(\mathbb{R}_+ \times [0, T^*])$.*

Note that the system (8) no longer depends on the term structure B, and thus the problem of identifying the volatility smile $A(Y)$ amounts to the identification of a time-independent volatility:

Inverse problem 2.1 (inverse smile problem). *Let $U_1(Y) := C(K, T^*)$ denote observed prices of European call options with maturity T^*. Find a function $A(Y)$ such that the solution $U(Y, \tau)$ of (8) satisfies*

$$U(Y, 1) = U_1(Y), \qquad Y \in \mathbb{R}_+. \tag{10}$$

We will summarize the main results in a stable regularized solution of this problem in section 3.

Once the volatility smile $A(\cdot)$ has been determined, the identification of the term structure $B(\cdot)$ can be performed by solving the following second inverse problem:

Inverse problem 2.2 (inverse term structure problem). *Let $U_2(T) := C(K^*, T)$ denote observed option prices for a fixed strike K^*, and $Y^*(T) := K^* e^{\int_0^T r(t)\,dt}$. Find a function $B(T)$ such that*

$$U\left(Y^*(T), \int_0^T B(t)\,dt\right) = U_2(T), \qquad T \in (0, T^*] \tag{11}$$

where $U = U_A$ denotes the solution of the Dupire equation (8) for a given smile A.

Note that the term structure B enters only via (7). We only mention that instead of $Y^*(T) = K^* e^{\int_0^T r(t)\,dt}$ other price trajectories, e.g. $Y^*(T) \equiv Y^*$ (at-the-money options), respectively all available option prices can be used for determining the term structure.

We now turn to a detailed discussion of the two inverse sub-problems 2.1 and 2.2, and investigate their stable solution by appropriate regularization methods.

3. On recovering the volatility smile

Identification of the volatility smile $A(Y)$ in (8) from option prices $U_1(Y)$ has been investigated previously, e.g. in [2, 3, 7, 11, 18]. For completeness of presentation and later reference, we recall the most important stability and uniqueness results for the inverse smile problem 2.1, and then discuss a stable approximate solution in the case of perturbed data via Tikhonov regularization.

The following uniqueness result for the inverse problem of determining $A(Y)$ from observations $U_1(Y)$ for $U(Y, 1)$ follows from results derived in [2, 3, 15]:

Proposition 3.1. *Let $U_{1,1}, U_{1,2}$ denote the solutions of (8) corresponding to parameter functions $A_1, A_2 \in C^\lambda(\overline{\mathbb{R}}_+)$ with $A_i(Y) \geqslant \underline{A} > 0$, and let $\Omega \subset \mathbb{R}_+$ denote an interval. If $A_1(Y) = A_2(Y)$ on a certain interval $\omega \subset \Omega$ and $U_{1,1}(Y, 1) = U_{1,2}(Y, 1)$ for $Y \in \Omega$, then $A_1(Y) = A_2(Y)$ on Ω. In case Ω is bounded, $0 \notin \overline{\Omega}$ and $A_1(Y) = A_2(Y)$ for $Y \in \mathbb{R}_+ \backslash \Omega$, then a Lipschitz estimate*

$$\|A_1(\cdot) - A_2(\cdot)\|_{C^\lambda(\Omega)} \leqslant C \|U_{1,1}(\cdot, 1) - U_{1,2}(\cdot, 1)\|_{C^{2+\lambda}(\Omega)},$$

holds.

If only perturbed data U_1^δ are available instead of U_1, then a solution A to the inverse problem

$$U(Y, 1) = U_1^\delta(Y), \qquad Y \in \mathbb{R}_+$$

will in general not exist. In order to overcome the problem of non-solvability, one can use a least-squares approach, which has additionally to be regularized, since the inverse problem is ill-posed. A stable solution of the inverse smile problem (10) formulated in logarithmic variables (cf (9)) via Tikhonov regularization has been investigated, e.g. in [4, 7, 18]. We shortly outline the key results.

Consider the Tikhonov functional

$$f(a) = \|u(\cdot, 1; a) - u_1^\delta\|_u^2 + \alpha \|a - a_0\|_a^2, \tag{12}$$

where a_0 denotes an appropriate initial guess and u_1^δ denote the perturbed data satisfying

$$\left\| u_1 - u_1^\delta \right\|_u \leqslant \delta \tag{13}$$

and $u_1(y) := u(y, 1; a^\dagger)$ are the noise free data corresponding to the true volatility $a^\dagger$. The existence of a minimizer a_α^δ of (12) has been shown for reasonable choices of norms $\|\cdot\|_u, \|\cdot\|_a$ and for the following set of admissible parameters,

$$\mathcal{K}_a^* = \{a \in a^* + H^1(\mathbb{R}) : 0 < \underline{a} \leqslant a \leqslant \overline{a}\}, \tag{14}$$

with $a^* \in \{a : 0 < \underline{a} \leqslant a \leqslant \overline{a}, \quad \nabla a \in L_2(\mathbb{R})\}$. The uniqueness of a minimizer for a sufficiently small time horizon τ^*, i.e. for $u_1(y) := u(y, \tau^*)$, follows from the following result derived in [18] if weighted norms are used in (12):

Proposition 3.2 (theorem 7.4 in [18]). *Assume that $a_1(y), a_2(y)$ are two minimizers of the Tikhonov functional*

$$f_\rho(a) = \|u(\cdot, \tau^*) - u_1^*(\cdot)\|_\rho^2 + \alpha \|\nabla a\|_\rho^2 \tag{15}$$

with norm $\|v\|_\rho^2 = \int_\mathbb{R} v(y) \rho(y) \, \mathrm{d}y$ and weight $\rho(y) \geqslant \rho_0 > 0$ such that $\int_\mathbb{R} \rho(y)^{-1} \, \mathrm{d}y < \infty$. If there exists a point y_0 such that $a_1(y_0) = a_2(y_0)$ and τ^* is sufficiently small, then $a_1 \equiv a_2$.

A careful inspection of the proofs in [18] shows that it is possible to choose $\tau^* = 1$ if ρ^{-1} decreases fast enough, and thus the result can be applied to our situation.

While for theoretical considerations it might be adequate to assume that observations are available for a continuum of strikes, this is of course not possible in reality, where only prices for a discrete set of strikes are quoted. In [7], both situations have been considered, and stability, convergence and convergence rates of the Tikhonov regularized solutions a_α^δ with vanishing noise $\|u - u^\delta\|_u \leqslant \delta \to 0$ have been shown. In the following let $\|\cdot\|_a := \|\cdot\|_{H^1(\mathbb{R})}$ and u be the solution to (9). Additionally, let $F : \mathcal{K}_a^* \to \mathcal{U}$ denote the mapping $F : a \mapsto u(y, 1)$ respectively $F : a \mapsto u(y_i, 1)$ with $\mathcal{U} = L_2(\mathbb{R})$ respectively $\mathcal{U} = \mathbb{R}^n$ and $\|\cdot\|_u$ be accordingly defined either by

$$\|u\|_u^2 = \int_\mathbb{R} |u(y, 1)|^2 \, \mathrm{d}y \qquad \text{or} \qquad \|u\|_u^2 = \sum_i u(y_i, 1)^2.$$

Proposition 3.3 (cf [7], theorems 3.1, 3.2; [8], theorem 10.4). *Let $\alpha > 0, u_1^k \to u_1^\delta$ and a_k denote the minimizer of (12) with u_1^δ replaced by u_1^k. Then there exists a convergent sub-sequence of $\{a_k\}$ and the limit of each convergent sub-sequence is a minimizer of (12).*

If (13) holds and $\alpha(\delta)$ is such that $\alpha(\delta), \delta^2/\alpha(\delta) \to 0$, then every sequence $\{a_k\}$, where $\delta_k \to 0$ and $a_k = a_{\alpha(\delta^k)}^{\delta_k}$ denotes a minimizer of (12) with u_1^* replaced by $u_1^{\delta_k}$ satisfying (13), has a convergent sub-sequence. The limit of every convergent sub-sequence is an a^*-minimum-norm solution.

The forward operator F is Fréchet differentiable on $\mathcal{K}_a^*$ and the derivative $F'(a^\dagger)$ satisfies a Lipschitz condition

$$\|[F'(a) - F'(a^\dagger)]b\|_u \leqslant L \|a - a^\dagger\|_a \tag{16}$$

locally around $a^\dagger$. If the a priori choice $a^* - a^\dagger \in \mathcal{R}(F'(a^\dagger)^*)$, i.e.

$$a^\dagger - a^* = F'(a^\dagger)^* w \tag{17}$$

and $\|w\|_u$ is sufficiently small, then with the choice $\alpha \sim \delta$ the rate

$$\left\| a_\alpha^\delta - a^\dagger \right\|_a = O(\sqrt{\delta}) \tag{18}$$

holds.

Note that in view of proposition 3.2 we expect the minimizers a_k to be unique if a complete set of option prices $u(y, 1)$ for all $y \in \mathbb{R}$ are available, in which case the convergence in the above proposition would hold in the strong sense. The rates (18) were proven in [7] under simpler conditions on $g := a^\dagger - a^*$, namely

$$|g^{(i)}| = O(\mathrm{e}^{-|y|}), \qquad i = 1, \ldots, 6 \text{ respectively } i = 1, \ldots, 4. \tag{19}$$

It was independently shown in [11] that similar decay conditions are necessary in order to show that $a^\dagger - a^* \in \mathcal{R}(F'(a^\dagger)^*)$. Note, that the condition (19) is actually quite similar to the requirement that $a(\cdot)$ has to be known outside of Ω for the stability result in proposition 3.1, i.e. the volatility $a(y)$ has to be known almost precisely for large $|y|$ in order to get good approximations.

By exploiting the definition $y = \log(Y)$, the above results carry over immediately to the formulation (10), (8) of the inverse smile problem 2.1 in natural variables if the following weighted norms are used:

$$\|U\|_U^2 = \int_{\mathbb{R}_+} |U(Y)|^2 \frac{1}{Y} \, dY, \qquad \|A\|_A^2 = \int_{\mathbb{R}_+} (|A(Y)|^2 + |Y \nabla_Y A(Y)|^2) \frac{1}{Y} \, dY. \tag{20}$$

We will use such weighted norms also in our numerical examples below.

4. Recovering the term structure

First, the identification of the term structure from option data corresponding to a known volatility smile A, cf inverse problem 2.2, will be discussed. At the end of this section, we then also investigate the case when A is only known approximately, e.g. from a prior identification of the smile (see section 3 and inverse problem 2.1).

For the moment let A be given and $U(Y, \tau)$ denote the solution of the Dupire equation (8). Let U_2, U_2^δ denote (measurements of the) option prices corresponding to strikes $Y^* := K^* \mathrm{e}^{\int_0^T r(t) \, dt}$ with $K^* > 0$, i.e.,

$$U(Y^*(T), \tau(T)) = U_2(T), \qquad T \in (0, 1) \tag{21}$$

and $\|U_2 - U_2^\delta\|_U \leq \delta$, where $\tau(T) = \int_0^T B(t) \, dt$ and $B(t)$ denotes the true term structure, which is to be determined from (21). Formally, this inverse problem can be written as

$$G(B) = U_2^\delta, \qquad [G(B)](T) = [G_A(B)](T) := U \left(Y^*(T), \int_0^T B(t) \, dt \right), \tag{22}$$

where we consider G as an operator from

$$\mathcal{D}(G) := \left\{ B \in L_2(0, 1) : 0 < \underline{B} \leq B, \int_0^1 B(t) \, dt = 1 \right\}$$

to $L_2(0, 1)$, and $Y^*(T) = \mathrm{e}^{\int_0^T r(t) \, dt} K^*$ is defined as above. We will write G_A only if the dependence of A is important. Note that in contrast to a comparable discussion in [12] the function U here is not explicitly available, but implicitly given as a solution to (8). For the subsequent analysis we will utilize the following properties of the mapping operator G:

Proposition 4.1. *The operator* $G : \mathcal{D}(G) \subset L_2(0, 1) \to L_2(0, 1)$ *is injective, compact, continuous and weakly closed. Moreover, if* $K^* \neq S_0$, *then for every* $B_0 \in \mathcal{D}(G)$ *there exists a linear bounded operator* $G'(B_0) : L_2(0, 1) \to L_2(0, 1)$ *such that*

$$\|G(B) - G(B_0) - G'(B_0)(B - B_0)\|_{L_2(0,1)} \leq \frac{L}{2} \|B - B_0\|_{L_2(0,1)}^2, \tag{23}$$

holds for all $B \in \mathcal{D}(G)$ *with L not depending on* B_0.

Proof. We decompose $G = N \circ J$, where the operators $J, N : L_2(0, 1) \to L_2(0, 1)$ are defined by $(JB)(T) := \int_0^T B(t)\,\mathrm{d}t$ and $N(\tau)(T) = U(Y^*(T), \tau(T))$. Note that $Y^2 U_{YY} = \Gamma(Y, \tau; S, 0)$ where Γ denotes a fundamental solution to (8) (see [3]), and hence $U_\tau > 0$ for $T > 0$. Thus G is the concatenation of injective operators. By the regularity of U (cf proposition 2.1) it follows that N is continuous, which together with the compactness of J yields the continuity and compactness of G. The weak closedness follows by noting that $\mathcal{D}(G)$ is a closed convex set. For the Taylor approximation (23) we use

$$[G(B) - G(B_0)](T) = \int_0^1 U_\tau \left(Y^*(T), \int_0^T (1-s)B(t) + s B_0(t)\,\mathrm{d}t\right)\,\mathrm{d}s \int_0^T B(t) - B_0(t)\,\mathrm{d}t$$

and that even $U_{\tau\tau}$ is bounded uniformly on $\mathbb{R}_+ \times [0, 1] \setminus \{(K, T) : |K - S_0| + |T| < |K_* - S_0|/2\}$. $\qquad\square$

Applying proposition A.3 and remark A.4 of [9], we conclude the local ill-posedness of equation (21) in the sense of [13 definition 2]:

Corollary 4.1. *For every $B \in \mathcal{D}(G)$ and every ball $B_r(B)$ with $r > 0$, there exists a sequence $\{B_n\} \subset \mathcal{D}(G) \cap B_r(B)$ with $B_n \rightharpoonup B$, $B_n \not\to B$ but $G(B_n) \to G(B)$. In particular, equation (21) is locally ill-posed and G^{-1} is not continuous in $G(B)$.*

For stabilization of the problem (21) we consider Tikhonov regularization, i.e. for noisy data U_2^δ and some regularization parameter $\beta > 0$, an approximate solution of (21) is defined via

$$\left\|G(B) - U_2^\delta\right\|_{L_2(0,1)}^2 + \beta \|B - B^*\|_{L_2(0,1)}^2 \to \min, \qquad B \in \mathcal{D}(G). \tag{24}$$

Utilizing proposition 4.1, standard results of regularization theory (cf [9]) yield that such a minimizer exists. If $\delta_n \to 0$ and $\delta_n^2/\beta_n \to 0$, then the regularized solutions $B_{\beta_n}^{\delta_n}$ converge to the true solution $B^\dagger$. Moreover, the following convergence rates result holds:

Proposition 4.2. *Let $B^\dagger$ denote the true solution of (21) and assume that there exists a function $w \in L_2(0, 1)$ such that*

(i) $B^\dagger - B^* = G'(B^\dagger)^* w$ with
(ii) $L\|w\|_{L_2(0,1)} < 1$,

where L is the constant of the estimate (23). Let B_β^δ denote the minimizer of (24) with $\beta \sim \delta$ then

$$\left\|B_\beta^\delta - B^\dagger\right\|_{L_2(0,1)} = O(\sqrt{\delta}).$$

Remark 4.1. For the problem under investigation, the source condition (i) can be interpreted in the following way, cf [12]. Let

$$m(T) := U_\tau \left(Y^*(T), \int_0^T B^\dagger(t)\,\mathrm{d}t\right), \qquad T \in (0, 1).$$

Then (i) is equivalent to

$$(B^\dagger - B^*)(0) = 0 \qquad \text{and} \qquad \frac{(B^\dagger - B^*)'}{m} \in L_2(0, 1).$$

Note that the denominator $m(0) = 0$ and $m(T) > 0$ for $T > 0$. Thus (i) is a stronger condition than $B^\dagger - B^* \in H^1(0, 1)$.

At the end of this section we will discuss the situation in which parameter A in the sub-problem (21) is only known approximately, which will be the typical situation in our decomposition approach:

Lemma 4.1. *For $A, \tilde{A} \in \mathcal{K}_a^*$, let $U, \tilde{U}$ denote the solutions of (8) and $G_A, G_{\tilde{A}}$ be defined as in (22). Then for $B \in \mathcal{D}(G)$ the estimate*

$$\|G_A(B) - G_{\tilde{A}}(B)\|_{L_2(0,1)} \leqslant C\|A - \tilde{A}\|_a$$

holds for a constant $C > 0$ independent of A, $\tilde{A}$ and B. Here, $\|\cdot\|_a$ denotes the norm defined by (20).

Proof. For the proof we utilize the formulation of the Dupire equation in logarithmic variables, cf (9). The difference $v := u - \tilde{u}$ then solves

$$v_\tau = a(y)(v_{yy} - v_y) + (a(y) - \tilde{a}(y))(\tilde{u}_{yy} - \tilde{u}_y), \qquad v(y, 0) = 0.$$

As shown in [7, 11], a solution to (9) has the regularity $u \in L^2(0, 1; H^2(\mathbb{R}))$, and the same regularity holds for v. Moreover,

$$\|v\|_{L_2(0,1;H^2(\mathbb{R}))} \leqslant \|a - \tilde{a}\|_{H^1(\mathbb{R})} \|\tilde{u}\|_{L_2(0,1;H^2(\mathbb{R}))}.$$

The result then follows by back-substitution to natural variables. $\qquad \square$

Proposition 4.3. *Let U_2 denote the true data corresponding to the inverse problem (22) with smile A and true solution $B^\dagger$. Assume that $\|U_2^\delta\|_{L_2(0,1)} \leqslant \delta$ and $\|A - \overline{A}\|_A \leqslant \delta_A$, where $\|\cdot\|_A$ denotes the norm defined in (20), and let $\overline{B}_\beta^\delta$ denote the minimizer of (24) with data U_2^δ, parameter $\overline{A}$, and $\beta \sim \sqrt{\delta_A} + \delta$. Then*

$$\left\|\overline{B}_\beta^\delta - B^\dagger\right\|_{L_2(0,1)}^2 = O(\sqrt{\delta_A} + \delta).$$

Proof. Using lemma 4.1 we have

$$\left\|G_A\big(\overline{B}_\beta^\delta\big) - U_2^\delta\right\|_{L_2(0,1)}^2 + \beta\left\|\overline{B}_\beta^\delta\right\|_{L_2(0,1)}^2 \leqslant C\delta^2 + 2\beta\big\langle B^\dagger - B^*, B^\dagger - \overline{B}_\beta^\delta\big\rangle_{L_2(0,1)}. \qquad (25)$$

The rest follows as in the proof of [8, theorem 10.4]. $\qquad \square$

Together with the convergence result for the inverse smile problem we obtain that under the conditions of propositions 3.2, 4.2 (with $\overline{A}$ replaced by A_α^δ) the following convergence rates hold,

$$\left\|A_\alpha^\delta - A^\dagger\right\|_A = O(\sqrt{\delta_A}) \qquad \text{and} \qquad \left\|\overline{B}_\beta^\delta - B^\dagger\right\|_{L_2(0,1)} = O\big(\sqrt{\sqrt{\delta_A} + \delta_B}\big),$$

where δ_A and δ_B denote the noise levels of the data U_1 and U_2, respectively, and the regularization parameters α, β are chosen appropriately, i.e. $\alpha \sim \delta_A$, $\beta \sim \sqrt{\delta_A} + \delta_B$.

5. Numerical aspects

In this section, we discuss several aspects of a numerical solution of the inverse problems 2.1, 2.2, and present the results of our numerical test.

Discretization of the forward problem. The option pricing equations (4), respectively (8), are discretized by finite differences in space and a Crank–Nicholson scheme in time. We have observed in our numerical experiments that the stability and accuracy of the solution of the Dupire equation is comparable for both formulations, (8) in natural variables, and (9) in logarithmic variables. Here, we stay with the natural variables and restrict the space domain

to $K \in [0, 5S]$ with appropriate Dirichlet boundary conditions on both sides. Already for a rough discretization of 200 equidistant points in space and 100 equidistant points in time, the maximal deviation of the numerically calculated option prices (occurring near $K = S$ and $T = 0$) is by a factor 10 less than the typical bid–ask spread (and thus the expected discrepancies) in the option prices of about 1% of S.

In order to illustrate that local volatility surfaces satisfying (5) can be stably identified by our approach, we consider the following test example:

Example 1. Let $S_0 = 1, T^* = 1, r = 7.5\%$ and $\sigma(K, T)$ have the form (5) with

$$A^\dagger(Y) = \tfrac{1}{20}\left[1 - \tfrac{1}{2}\exp(-4\log^2(Y)) \cdot \sin(2\pi Y)\right] \tag{26}$$

and

$$B^\dagger(T) = 1 + \tfrac{3}{5}\sin(2\pi T). \tag{27}$$

We try to identify A and B from option price data C_i^* for $T^* = 1$ and $K_i = 0.6 + i0.05 \in$ [0.6, 2], respectively C_j^* with $K^* = S_0 = 1$ and $T_j = 0.1 + j * 0.1 \in [0.1, 1]$. The option prices C_i^*, C_j^* corresponding to (26), (27) are computed numerically according to (4) and additionally perturbed by uniformly $[-\delta, \delta]$ distributed random noise. In accordance to the expected errors in observed option prices, we set $\delta = 10^{-3}$.

The values for T^*, r and A are motivated by the following consideration. Assume that option prices with maturities for the next two and a half years are available, the interest rate is about 2.5% and the volatility of the underlying is about 20%. By a rescaling of time, we get $T^* = 1, r \sim 7.5\%$, and $\sigma^2 \sim 0.1$. The T_j then correspond to quarter–annual expiries.

Identification of the volatility smile. As outlined in section 2, we first reconstruct the volatility smile $A(Y)$ from option prices C_i^* for the maturity T^* and strikes K_i, which are discounted according to $Y_i = K_i \, e^{-rT^*}$. In analogy to section 3 we define the regularized solution as the minimizer of the Tikhonov functional

$$\frac{1}{N_i}\sum_{i=1}^{N_i}|C_i^* - U(Y_i, 1)|^2 + \alpha\|A - A^*\|_*^2, \tag{28}$$

where $U(Y, \tau)$ denotes the solution to (8) restricted to the domain $(y, \tau) \in (0, 5) \times (0, 1)$. For regularization, we use the norm

$$\|A\|_*^2 = \int_0^5 A(Y)^2 \frac{1}{Y}\,\mathrm{d}Y + \int_0^5 A_Y(Y)^2 Y\,\mathrm{d}Y \tag{29}$$

which amounts to the H^1 norm of $a(y) := A(Y)$ in logarithmic variables $y = \log(Y)$; see section 3. The stability and convergence results cited in section 3 are directly applicable and yield convergence (in a set-valued sense) of the regularized solutions to an A^*-minimum-norm solution. The regularization parameter α is determined by a discrepancy principle, i.e. we start with α_0 and decrease α until the residual $\max\{|C_i^* - U(Y_i, 1)|\} \leqslant \tau\delta$.

The minimization of the Tikhonov functional (28) is carried out by a Newton–CG algorithm [10]. For $\alpha = \alpha_0$, the algorithm is started at the *a priori* guess A^*, yielding a minimizer $A_{\alpha_0}^\delta$ and for $\alpha = \alpha_i := 2^{-i}\alpha_0$ the iteration is then started at the previous minimizer $A_{\alpha_{i-1}}^\delta$. In each Newton step, a CG iteration is applied for the solution of the linearized equation. The inner (CG) iteration is stopped, when the residual of the linearized equation has been decreased by a constant factor q (we choose here $q = 0.5$). If the *a priori* guess is assumed not to reflect the asymptotic behaviour (for Y large/small), one might also use the Newton–CG algorithm directly as regularization method (see, e.g., [10]), in which case the volatility function does not stay so close to the initial guess A^* as in the case of Tikhonov
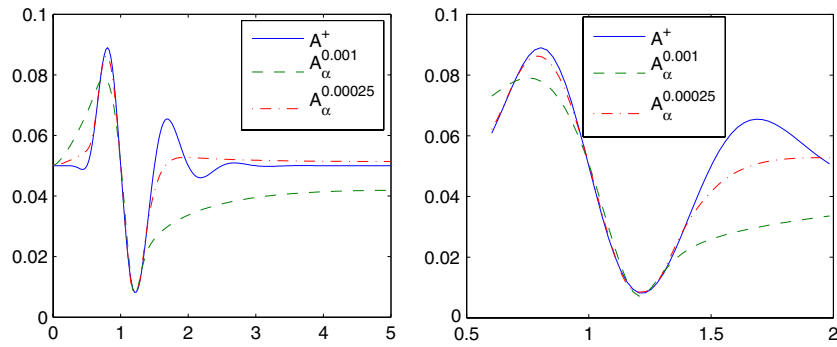
Figure 1. The true smile $A^\dagger$ and the reconstructions A_α^δ for $\delta = 0.001$ and $\delta = 0.00025$ (cf table 1).

Table 1. Convergence rates for the inverse smile problem, example 1.

δ	$\frac{\|C_i^* - U_i(A_\alpha^\delta\|)}{\|C_i^* - U_i(A^*)\|}$	$\frac{\|A_\alpha^\delta - A^\dagger\|}{\|A^* - A^\dagger\|}$	it$_{\text{New}}$(it$_{\text{CG}}$)	α
0.004	0.3689	0.7680	2 (3)	0.001
0.002	0.2030	0.6027	3 (5)	0.001
0.001	**0.1429**	**0.5588**	**4 (10)**	**0.001**
0.0005	0.0703	0.3921	9 (34)	0.00025
0.00025	0.0252	0.3377	10 (46)	6.25×10^{-5}

regularization. The computational effort for one Newton step with N inner CG iterations essentially consists of $2(N + 1)$ solutions of (8) or the linearized (adjoint) equation. The numerically observed convergence rate is $\|A^\dagger - A_\alpha^\delta\| \sim \delta^{0.30}$. In view of the results cited in section 3 we expect a good approximation of the volatility smile only in the region where option prices are observed. Additionally, the quality of the reconstructions will decrease rapidly for large/small strikes. Both effects are also observed in the numerical test; cf figure 1.

We mention that even if the *a priori* guess has the wrong asymptotic behaviour, the reconstructions in the region of interest are still comparably good.

Identification of the term structure. The second part of our numerical test cf figure 2, table 2 consists of identifying the term structure $B(T)$ from option prices corresponding to a single strike price K^* and several maturities T_j given (at least an estimate for) the volatility smile $A(Y)$. As we have seen in section 2, the prices for maturity T_j do not depend on $B(T)$ but only on $\int_0^{T_j} B(t)\, dt$, i.e. in the case of only few observations the problem is highly underdetermined and uniqueness (and stability) of a solution has to be enforced by some kind of regularization. Taking into account the specific data situation, we choose the Tikhonov functional

$$\frac{1}{N_T} \sum_{j=1}^{N_T} |C^*(K^*, T_j) - U(K^* e^{-rT_j}, \tau(T_j))|^2 + \beta \|\tau - \tau^*\|_{H^1}^2 \tag{30}$$

instead of (24). Note that by (7) we have $\tau(0) = 0$ and $\tau(1) = 1$. Thus the regularization term $\|\tau - \tau^*\|_{H^1}^2$ is equivalent to $\|B - B^*\|_{L^2}^2$ in (24). Once τ has been determined as the minimizer of (30), the term structure $B(T)$ can be found by differentiating τ which is a stable operation from H^1 to L_2. For minimizing the Tikhonov functional and the parameter choice the same algorithms as for the inverse smile problem above can be used. The solution can be further improved if data for several price trajectories, e.g. all available option prices,
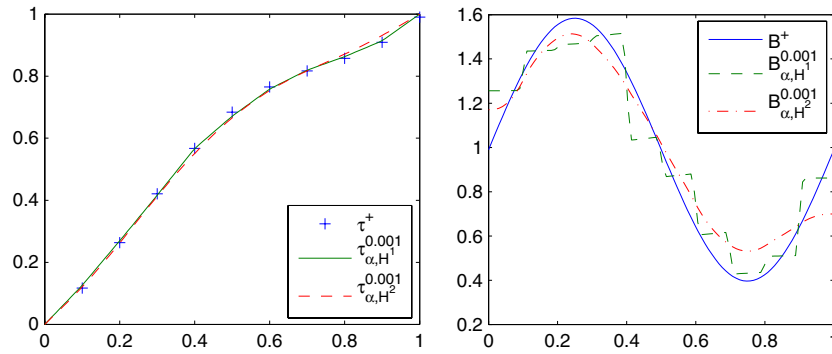
Figure 2. Left: the true maturities τ^δ and the regularized approximations τ_α^δ for H^1 and H^2 regularization. Right: the underlying term structure $B^\dagger$ and the corresponding reconstructions B_α^δ (cf table 2).

Table 2. Convergence rates and iteration numbers (inner/outer iterations) for the inverse term structure problem.

δ	$\frac{\|C^*-U(B_\alpha^\delta)\|}{\|C^*-U(B_0)\|}$	$\frac{\|B_\alpha^\delta-B^\dagger\|}{\|B^*-B^\delta\|}$	it$_{\text{New}}$(it$_{\text{CG}}$)
0.00 4	0.001 031	0.031 95	1 (4)
0.00 2	0.000 853	0.017 50	1 (4)
0.00 1	**0.000 837**	**0.014 45**	**1 (3)**
0.000 5	0.000 290	0.009 20	2 (8)
0.000 25	0.000 233	0.007 45	2 (7)

are taken into account. In this case, the least-squares term reads

$$\frac{1}{N_T}\sum_{j=1}^{N_T}\frac{1}{N_{K,j}}\sum_{i=0}^{N_{K,j}}|C^*(K_{ij}^*, T_j) - U(K_{ij}^*\,\mathrm{e}^{-rT_j}, \tau(T_j))|^2.$$

In our example, the inverse problem is already regularized sufficiently by discretization (only 10 maturities) and we can set $\beta = 0$. If data for more maturities are available, β can be chosen in a similar manner as α was chosen for determining the smile structure above, which slightly increases the numerical effort.

Note that for sparse data, the minimizer of the Tikhonov functional (30) is a piecewise linear function, and thus the term structure $B(T)$ is piecewise constant here. The smoothness of the solution can be enforced by regularizing in a stronger norm, e.g. H^2 yields a piecewise linear term structure $B(T)$. On the other hand, this shows that a solution B to the inverse term structure problem is not unique if only discrete data are available.

Finally, we remark that the inverse term structure problem is almost linear, i.e. we have

$$[G'(B)H](T) = U_\tau(K^*\,\mathrm{e}^{-rT}, B(T))H(T).$$

Thus the nonlinearity is essentially determined by the deviation of U_τ from a constant, which is usually not too large if T is not too small. This weakly nonlinear behaviour is also observed in the numerical tests, where only 1 or 2 Newton iterations are needed for a reasonable minimization of (30).

Identification of non-conforming volatility surfaces. As we have illustrated above, volatility surfaces of the form (5) can be efficiently reconstructed by our approach. If, however,

the true volatility does not satisfy the assumption (5), another technique is needed to fully calibrate the model to the market. Still, our approach can be used to construct a good initial guess for the full calibration problem, which might be formulated as minimization of

$$\frac{1}{N_T} \sum_{j=1}^{N_T} \frac{1}{N_{K,j}} \sum_{i=0}^{N_{K,j}} |C^*(K_{ij}^*, T_j) - C(K_{ij}^*, T_j)|^2 + \alpha \|\sigma^2 - \sigma_*^2\|^2, \tag{31}$$

where $\sigma_*^2(K, T) := 2A_\alpha^\delta(Y) B_\alpha^\delta(T)$ with $A_\alpha^\delta(Y)$ and $B_\alpha^\delta(T)$ determined as described above. For a detailed discussion of the full calibration problem, we refer to [4, 7, 16, 17] and the references cited therein.

Acknowledgment

References

[1] Black F and Scholes M 1973 The pricing of options and corporate liabilities *J. Polit. Econ.* **81** 637–59
[2] Bouchouev I and Isakov V 1997 The inverse problem of option pricing *Inverse Problems* **13** L1–L7
[3] Bouchouev I and Isakov V 1999 Uniqueness, stability and numerical methods for the inverse problem that arises in financial markets *Inverse Problems* **15** R95–R116
[4] Crépey S 2003 Calibration of the local volatility in a generalized Black–Scholes model using Tikhonov regularization *SIAM J. Math. Anal.* **34** 1183–206
[5] Derman E and Kani I 1994 Riding on a smile *RISK* **7** 32–9
[6] Dupire B 1994 Pricing with a smile *RISK* **7** 18–20
[7] Egger H and Engl H W 2005 Tikhonov regularization applied to the inverse problem of option pricing: convergence analysis and rates *Inverse Problems* **21** 1027–45
[8] Engl H W, Hanke M and Neubauer A 1996 *Regularization of Inverse Problems* (Dordrecht: Kluwer)
[9] Engl H W, Kunisch K and Neubauer A 1989 Convergence rates for Tikhonov regularisation of non-linear ill-posed problems *Inverse Problems* **5** 523–40
[10] Hanke M 1997 Regularizing properties of a truncated Newton–CG algorithm for nonlinear inverse problems *Numer. Funct. Anal. Optim.* **18** 971–93
[11] Hein T 2005 Some analysis of Tikhonov regularization for the inverse problem of option pricing in the price-dependent case *J. Anal. Appl.* **24** 593–610
[12] Hein T and Hofmann B 2003 On the nature of ill-posedness of an inverse problem in option pricing *Inverse Problems* **19** 1319–38
[13] Hofmann B and Scherzer O 1994 Factors influencing the ill-posedness of nonlinear problems *Inverse Problems* **10** 1277–97
[14] Hull J 2000 *Options, Futures, and Other Derivatives* 4th edn (Englewood Cliffs, NJ: Prentice-Hall)
[15] Isakov V 2003 The inverse problem of option pricing *Recent Development in Theories & Numerics—Int. Conf. on Inverse Problems* ed Y-Ch Hon, M Yamamoto, J Cheng and J-Y Lee (Singapore: World Scientific) pp 47–55
[16] Jackson N, Süli E and Howison S 1998 Computation of deterministic volatility surfaces *J. Math. Finance* **2** 5–32
[17] Lagnado R and Osher S 1997 A technique for calibrating derivative security pricing models: numerical solution of the inverse problem *J. Comput. Finance* **1** 13–25
[18] Lishang J and Youshan T 2001 Identifying the volatility of underlying assets from option prices *Inverse Problems* **17** 137–55
[19] Wilmott P, Dewynne J and Howison S 1995 *The Mathematics of Financial Derivatives* (Cambridge: Cambridge University Press)
[20] Zubelli J P 2005 Inverse problems in finance: A short survey of calibration techniques *Proc. 2nd Brazilian Conf. on Statistical Modelling in Insurance and Finance (Maresias, Brazil)* ed N Kolev and P Morettin pp 64–75 (Institute of Mathematics and Statistics, University of São Paulo)